JOURNAL OF VIROLOGY, Nov. 2008, p. 11152–11166 Vol. 82, No. 22
0022-538X/08/$08.00+0 doi:10.1128/JVI.01519-08

Multiple Virus Lineages Sharing Recent Common Ancestry Were Associated with a Large Rift Valley Fever Outbreak among Livestock in Kenya during 2006-2007▽†

Brian H. Bird,[1,4] Jane W. K. Githinji,[3] Joseph M. Macharia,[3] Jacqueline L. Kasiiti,[3] Rees M. Muriithi,[3] Stephen G. Gacheru,[3] Joseph O. Musaa,[3] Jonathan S. Towner,[1] Serena A. Reeder,[1] Jennifer B. Oliver,[1] Thomas L. Stevens,[1] Bobbie R. Erickson,[1] Laura T. Morgan,[1] Marina L. Khristova,[2] Amy L. Hartman,[1] James A. Comer,[1] Pierre E. Rollin,[1] Thomas G. Ksiazek,[1] and Stuart T. Nichol[1]*

Special Pathogens Branch, Division of Viral and Rickettsial Diseases, Coordinating Center for Infectious Diseases,[1] and Biotechnology Core Facility Branch,[2] Centers for Disease Control and Prevention, 1600 Clifton Road MS G-14, Atlanta, Georgia 30329; Ministry of Livestock and Fisheries Development, Department of Veterinary Services, Kabete, Kenya[3]; and University of California, Davis, School of Veterinary Medicine, Davis, California 95616[4]

Received 18 July 2008/Accepted 27 August 2008

Rift Valley fever (RVF) virus historically has caused widespread and extensive outbreaks of severe human and livestock disease throughout Africa, Madagascar, and the Arabian Peninsula. Following unusually heavy rainfall during the late autumn of 2006, reports of human and animal illness consistent with RVF virus infection emerged across semiarid regions of the Garissa District of northeastern Kenya and southern Somalia. Following initial RVF virus laboratory confirmation, a high-throughput RVF diagnostic facility was established at the Kenyan Central Veterinary Laboratories in Kabete, Kenya, to support the real-time identification of infected livestock and to facilitate outbreak response and control activities. A total of 3,250 specimens from a variety of animal species, including domesticated livestock (cattle, sheep, goats, and camels) and wildlife collected from a total of 55 of 71 Kenyan administrative districts, were tested by molecular and serologic assays. Evidence of RVF infection was found in 9.2% of animals tested and across 23 districts of Kenya, reflecting the large number of affected livestock and the geographic extent of the outbreak. The complete S, M, and/or L genome segment sequence was obtained from a total of 31 RVF virus specimens spanning the entire known outbreak period (December-May) and geographic areas affected by RVF virus activity. Extensive genomic analyses demonstrated the concurrent circulation of multiple virus lineages, gene segment reassortment, and the common ancestry of the 2006/2007 outbreak viruses with those from the 1997-1998 east African RVF outbreak. Evidence of recent increases in genomic diversity and effective population size 2 to 4 years prior to the 2006-2007 outbreak also was found, indicating ongoing RVF virus activity and evolution during the interepizootic/epidemic period. These findings have implications for further studies of basic RVF virus ecology and the design of future surveillance/diagnostic activities, and they highlight the critical need for safe and effective vaccines and antiviral compounds to combat this significant veterinary and public health threat.

Rift Valley fever (RVF) virus historically has been responsible for large explosive outbreaks of severe human and animal disease throughout Africa and, in 2000, the Arabian Peninsula (12). The continued medical and veterinary importance of this mosquito-borne virus was again highlighted during the later part of 2006 and early 2007, when a large epizootic-epidemic occurred in northeastern Africa (9). RVF virus outbreaks among livestock are economically devastating and often characterized by large sweeping abortion storms and significant mortality in adult livestock (primarily sheep, goats, and cattle), with newborn animal mortality approaching 100% (11, 15). The majority of human infections result in a mild to moderate self-limiting febrile illness of short duration. However, in a small percentage (~1 to 2%) of patients, the disease can progress to more serious complications, including acute hepatitis, encephalitis, retinitis, or a hemorrhagic syndrome, with a hospitalized case fatality of ~10 to 20% (34, 36, 37).

Although low-level RVF virus transmission likely occurs within enzootic regions each year, the emergence of virus activity in large epizootic-epidemic cycles is periodic and associated with abnormally high rainfall events that allow for the abundant emergence of *Aedes* species floodwater mosquitoes transovarially infected with RVF virus and secondary vectors (9, 29–31). These mosquitoes are thought to initiate outbreaks among livestock, particularly susceptible breeds of sheep and cattle. Human infections follow as the result of either direct mosquito transmission or from percutaneous/aerosol routes during the handling of aborted fetal materials or the slaughtering of infected livestock. The acute onset of large numbers of affected individuals and livestock during outbreaks can greatly strain public health and veterinary infrastructures.

Beginning in October of 2006 and continuing through December, heavy rainfall was recorded in the semiarid regions of south-

* Corresponding author. Mailing address: Special Pathogens Branch, Division of Viral and Rickettsial Diseases, Coordinating Center for Infectious Diseases, Centers for Disease Control and Prevention, 1600 Clifton Road, MS G-14, Atlanta, GA 30329. Phone: (404) 639-1115. Fax: (404) 639-1118. E-mail: stn1@cdc.gov.

† Supplemental material for this article may be found at http://jvi.asm.org/.

▽ Published ahead of print on 10 September 2008.

ern Somalia and northeastern Kenya (http://www.cpc.noaa.gov/). This rainfall resulted in dramatic flooding in these areas and early warning reports of an increased risk of RVF virus activity throughout eastern Africa (2 and http://www.geis.fhp.osd.mil/GEIS/SurveillanceActivities/RVFWeb/indexRVF.asp). The first reports of unexplained febrile illness among humans emerged in the Garissa District of the northeastern province of Kenya during mid-December 2006 (9). RVF virus infection among symptomatic humans and livestock subsequently was confirmed by the medical and veterinary authorities within Kenya. To assist in the rapid and high-throughput identification and surveillance of infected livestock throughout the country, a diagnostic laboratory employing both molecular and serologic assays was quickly established at the Ministry of Livestock and Fisheries, Central Veterinary Services Laboratories, in Kabete, Kenya.

While the initial focus of RVF virus activity occurred during December 2006 after heavy rains in the northeastern region of Kenya and southern Somalia, further widespread RVF virus cases subsequently were reported in central, southern, and western regions of Kenya and further south into central Tanzania as the heavy rainfall event shifted toward the south and west (http://www.cpc.noaa.gov/ and http://www.geis.fhp.osd.mil/GEIS/SurveillanceActivities/RVFWeb/indexRVF.asp). During the epidemic period (December 2006-May 2007), a total of 684 human cases and 155 deaths were reported in Kenya, with a further 114 cases and 51 deaths in Somalia and 264 cases and 109 deaths reported in Tanzania (1). Furthermore, in Kenya alone, official estimates of total livestock production potentially impacted directly or indirectly by the RVF virus epizootic include an estimated 9 million native-zebu breed cattle, 3.5 million exotic-European breed cattle, 8 million sheep, 11 million goats, and 850,000 camels (http://www.communication.go.ke/ministry.asp?ministryid=14).

The RVF virus genome (approximately 11.9 kb) is comprised of three negative-sense, single-stranded RNA segments (S, M, and L). Like other members of the genus *Phlebovirus*, the ambisense S segment encodes the nucleoprotein (NP) in the antigenomic sense and the nonstructural (NSs) protein in the genomic sense (47). The NSs protein functions in host cell transcription shutoff and the blocking of the host cell interferon response (28). The M segment encodes several viral proteins in a single open reading frame, including the 14-kDa NSm, two major envelope surface glycoproteins (Gn and Gc), and a 78-kDa fusion of NSm and Gn (51). The NSm proteins recently were shown to be nonessential for in vitro virus growth (22, 59) and shown to contribute to mammalian host virulence (4, 60). The L segment encodes the virus polymerase (47).

We report here results from the laboratory testing of over 3,000 specimens from livestock (cattle, sheep, goats, and camels) and wildlife collected throughout Kenya as part of efforts to survey the extent of the RVF outbreak and identify acutely infected animals. In addition to molecular and serologic testing, complete RVF virus genome sequences were determined and analyzed to provide the first comprehensive high-resolution examination of inter- and intraoutbreak RVF virus genomics and to highlight the dynamic nature of RVF virus ecology and evolution.

MATERIALS AND METHODS

Specimen collection and handling. Animal specimens were submitted to the Kenyan Ministry of Livestock and Fisheries, Central Veterinary Laboratories, in Kabete, Kenya, by following established Kenyan government policies. In response to the RVF virus outbreak, a diagnostic laboratory with both molecular and serologic capabilities was quickly established inside the virology unit diagnostic building. Each specimen received a unique identification number, and relevant data such as the date of collection, location of origin, species, approximate age, and Kenyan Veterinary Services identity number were recorded. To reduce the potential for cross-contamination, individual rooms were utilized for specimen sorting, specimen inactivation, total RNA extraction, quantitative reverse transcription-PCR (qRT-PCR) master mix setup, qRT-PCR amplification, and serologic testing. At all times, laboratory personnel utilized universal precaution techniques while conducting sample inventories and handling potentially infectious specimens. The processing and aliquoting of samples (serum, whole blood, or tissue) was performed using N-95 respiratory masks or powered air-purifying respirators under field conditions or in a laminar-flow biosafety cabinet. One serum or whole-blood aliquot was placed directly into 300 μl of virucidal lysis buffer (2× NC lysis buffer; Applied Biosystems) for qRT-PCR analysis, and a duplicate aliquot was utilized for RVF virus antigen capture and immunoglobulin M (IgM) and IgG enzyme-linked immunosorbent assays (ELISA). Animal tissue samples (~100 mg) were ground in 500 μl sterile phosphate-buffered saline, pH 7.2 (Gibco), using a ball bearing maceration shaker (GenoGrinder2000; OPS Diagnostics), and 50 μl of resulting slurry was transferred into 300 μl of 2× NC lysis buffer (Applied Biosystems) by following techniques described previously (54, 55, 56). The remaining blood or tissues samples were stored for later use in either −40°C freezers or in liquid nitrogen. With permission from the Kenyan government and under USDA permit, sera, tissues, and extracted total RNA identified as positive for RVF virus were transported in liquid nitrogen vapors in International Airline Transport Association-compliant safety dry shippers to the biosafety level 4 laboratory at the Centers for Disease Control and Prevention in Atlanta, GA, where they were inventoried and stored in liquid nitrogen for later virus isolation attempts under appropriate containment conditions.

RVF virus qRT-PCR. The molecular detection of RVF virus RNA was performed as previously described (5). To minimize potential cross-contamination, all enzyme reaction master mixes were prepared in a positive-flow HEPA-filtered PCR hood.

RVF virus serologic assays. RVF virus-specific antigen capture and IgM and IgG ELISAs were performed essentially as described previously (34). Following heat and detergent inactivation, specimens (serum or whole blood) were tested by RVF virus antigen capture assays and anti-RVF-specific IgM and IgG ELISA. RVF virus antigen capture assays were performed on 4 dilutions of the diagnostic material (1/4, 1/16, 1/64, and 1/256), with anti-RVF virus-specific IgM and IgG ELISAs completed using inactivated RVF virus-infected Vero E6 cell antigens and tested using 4 dilutions of each specimen (1/400, 1/1,600, 1/6,400, and 1/25,600). Titers and the cumulative sum of optical densities of each dilution (SUM_{OD}) minus the background absorbance of uninfected control Vero E6 cells (adjusted SUM_{OD}) were recorded. Specimens were considered positive only if both the adjusted SUM_{OD} and titer were above preestablished conservative cutoff values, which were set for antigen capture ELISA (≥0.45 and ≥1/16), IgM ELISA (≥0.75 and ≥1/1,600), and IgG ELISA (≥1.5 and ≥1/1,600).

RVF virus RT-PCR and complete genome sequencing. Total RNA obtained directly from clinical specimens or after virus isolation on Vero E6 cells was amplified by conventional RT-PCR (Superscript III Platinum *Taq* HIFI polymerase; Invitrogen) by following protocols previously described (6). For sequencing, a total of 21, 52, and 50 sequencing primers were used for the S, M, and L segments, respectively. Some additional strain-specific sequencing primers were used to cover difficult-to-sequence regions. Approximately 140 to 150 reads were obtained for each genome, resulting in an average sixfold redundancy at each base position.

Phylogenetic analyses. Sequence datasets were analyzed using Geneious (BioMatters), Seaview (21), the MAFFT alignment program (24), and the PAUP* program, version 4.0b10 (Sinauer Associates, Inc., Sunderland, MA). For phylogenetic analyses, appropriate nucleotide substitution models were selected using Modeltest/Modelscore v3.7 and Akaike's information criterion (41). Further analyses utilized the Bayesian analysis software packages BEAST v1.4.7, BEAUTi v1.4.7, and Tracer v1.4 (13) and Mr. Bayes v3.1.2 (44). Final Bayesian analyses were completed with a randomly generated starting-tree topology with priors including a GTR+Gamma nucleotide substitution model, relaxed uncorrelated logarithmic normal molecular clock, and Bayesian skyline tree priors, as well as a combined MCMC (Markov chain Monte Carlo) chain length of 9.0 ×

10^7 with a 2.25×10^7 burn in (i.e., 25% of the overall chain length). The choice of molecular clock and tree prior settings were determined by comparisons of various models within BEAST v1.4.7/TRACER v1.4 using calculated likelihood-score Bayes factors as the selection criterion (49, 50). To compare models, a total of three independent MCMC runs of 3.0×10^7 steps, starting from a random tree topology, were combined (LogCombiner v1.4.7) and analyzed on the basis of Bayes scores (Tracer v1.4) calculated from the marginal likelihood posterior data. To ensure that the analyses had sampled the available tree space, individual runs were completed three to five independent times, starting with random tree topologies, and the results were analyzed by the software package AWTY (40) to confirm posterior convergence and that the overall MCMC chain lengths were appropriate. Statistical support values for individual phylogenetic nodes are indicated by integers above each tree branch and represent the percent highest posterior density values (% HPD; i.e., 1.0 = 100% posterior support). Estimates of the time to the most recent common ancestor (TMRCA), in years prior to the date of collection of the most contemporary virus specimen, are indicated below each tree branch node.

Population genetics-based determination of distinct RVF virus lineages and detection of virus population expansion. Nucleotide sequences were collapsed into unique haplotypes, and a minimum spanning network (MSN) based on a 95% connection limit was created for each segment in TCS version 1.21 (10). Based on those results, mismatch distributions were generated, and Harpending's raggedness index was calculated to assess the evidence of recent demographic or spatial expansion (43). The timing of any potential population expansion event was calculated using the formula $t = \tau/2\mu l$, where μ is the mutation rate in terms of substitutions/site/year and l is the length of the nucleotide sequence. Additional tests of selective neutrality that are particularly sensitive to population expansions or bottlenecks, Fu's Fs (20) and Tajima's D (53) tests, were performed along with estimations of nucleotide diversity using Arlequin version 3.11 (19).

Analyses of intraoutbreak geographic and temporal correlation with RVF virus genetic diversity. Distance matrices were constructed for the genetic, geographic, and temporal data collected during the outbreak to look for patterns of isolation by distance (geographic versus genetic distance) or isolation over time (temporal versus genetic distance). Genetic distance matrices were generated for each segment in PAUP*4.0b10 (Sinauer Associates) using uncorrected *P* values. Geographic distances were calculated by designating a central point within the Kenyan administrative subdistrict in which a sample was collected, recording the latitude/longitude coordinates associated with that point, and subsequently taking the straight-line distances between all pairs of samples. Temporal distances were calculated using the collection date of each virus sample. Mantel tests and partial Mantel tests with 10,000 permutations were performed in XLSTAT (AddinSoft) to examine relationships between the genetic distance matrices of interest.

Virus segment sequence accession numbers. The sequences for the S, M, and L segments have been deposited in GenBank under accession numbers EU574057 to EU574087, EU574031 to EU574056, and EU574004 to EU574030, respectively.

RESULTS

Specimen collection, testing, and comparisons of assay performance (qRT-PCR and antigen capture, IgM, and IgG ELISAs). A total of 3,250 specimens (serum, whole blood, or tissue) were tested from individual animals collected from 55 of 71 Kenyan administrative districts (Fig. 1, Table 1). These specimens were collected over a 6-month period, with the earliest specimens collected in the Garissa District during December 2006. Of these, the majority were obtained from livestock species, including 1,226 bovine, 1,181 caprine, 641 ovine, and 110 camel specimens (Table 1). A small number of wildlife specimens (a total of 92) also were tested. Evidence of RVF virus infection was detected (by either molecular or serologic assay) in 9.2% (289/3,250) of the specimens tested, with positive animals being found in 38 of the 55 administrative districts sampled (Table 1).

An earlier study had shown that the RVF virus-reactive IgM antibody duration is relatively short (39). In that study, 73% of cattle were IgM negative by 2 months after acute infection, and all were negative by 6 months. Given the duration of this current RVF virus epizootic within Kenya from approximately November 2006 to May 2007, we characterize animals that were found to be RVF virus specific by PCR, antigen capture positive, and/or IgM antibody positive as recently infected (i.e., infected during the recognized time frame of this outbreak). Animals that were RVF virus IgG positive but IgM negative were characterized as past infections (i.e., animals that could have been infected in the early phase of this epizootic or prior to the recognition of this disease episode). In our study, approximately 56.4% of RVF virus-positive animals showed evidence of recent acute infection, whereas the other 43.6% were only IgG positive, indicating virus infection had likely occurred approximately 2 or more months prior to sampling (Table 1).

Comparisons of the performance of each diagnostic modality (qRT-PCR and antigen capture, IgM, and IgG ELISAs) were completed (Fig. 2). As expected, the qRT-PCR assay (5) was more sensitive in the detection of the early acute viremia/RNAemia phase of infection than antigen capture ELISA, with a total of 17 specimens that were identified as antigen capture ELISA negative but qRT-PCR positive (Fig. 2A). This difference seen with early-acute-phase samples likely reflects the higher intrinsic sensitivity of qRT-PCR in combination with the masking of antigenic epitopes following the early induction of host anti-RVF virus IgM and the lack of ELISA-detectable RVF virus antigen in later samples.

While the qRT-PCR assay is highly sensitive, it appears that the level of virus in the blood is greatly reduced as RVF virus-specific IgM and IgG levels rise. Of 163 acute-phase RVF virus-positive cases, only 3 were found to have RVF virus RNA levels that were detectable after becoming anti-RVF virus-specific IgM positive (Fig. 2B). As expected, no animals with detectable anti-RVF virus IgG were qRT-PCR positive (Fig. 2C). The majority (76%) of acute-phase-infected animals were identified by a positive anti-RVF virus-specific IgM result alone, with only 24% identified solely by qRT-PCR (Fig. 2B and D).

In addition to livestock species, evidence of RVF virus infection also was found in the small sample of buffalo and giraffe tested (Table 1). The RVF virus antigen detection and RT-PCR assays are species independent; however, the format of the IgM and IgG assays is such that antibodies from different species may be detected with different efficiencies. While we know the current assay performs well with livestock species such as cattle, sheep, and goats (26, 34, 35), the IgM and IgG assays have not been validated with other species such as camels or wildlife, so negative results with these species should be interpreted with caution. RVF virus-specific IgG positives were found in camels (23/110) and giraffe (3/7), and IgM positives were found in buffalo (Table 1). These initial data suggest that a larger survey of wildlife (with appropriately validated assays) is warranted to more clearly determine the potential wildlife involvement in RVF virus epizootic and interepizootic periods.

Complete RVF virus genome sequencing reveals evidence of multiple RVF virus lineages and RNA segment reassortment during the 2006-2007 epizootic. A total of 31 specimens were suitable for single-step RT-PCR amplification of whole-genome segments either from total RNA extracted directly from

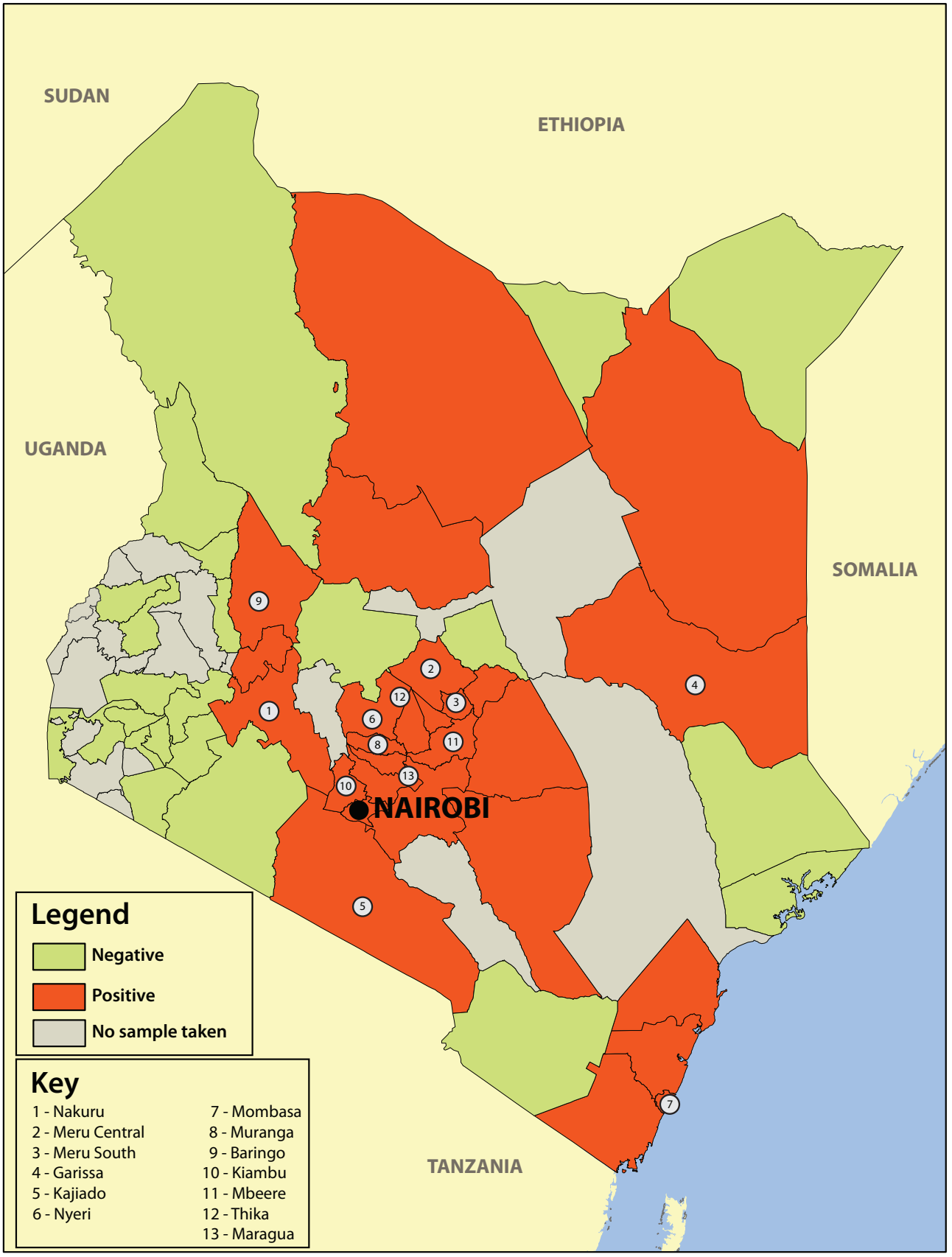

FIG. 1. Administrative district-level map of the Republic of Kenya. Shaded in red are districts in which evidence of acute-phase infection (by qRT-PCR, RVF virus antigen capture ELISA, and/or anti-RVF virus-specific IgM ELISA) was found.

TABLE 1. Summary of diagnostic testing

Species	Total no. of samples tested	No. of acute cases (by antigen or IgM ELISA and/or PCR)	No. of subacute cases (by IgG ELISA only)	Total no. positive
Bovine (*Bos* spp.)	1,226	72	42	114
Buffalo (*Syncerus caffer*)	26	4	0	4
Camel (*Camelus dromedarius*)	110	0	23	23
Caprine (*Capra hircus*)	1,181	39	41	80
Eland (*Tragelaphus oryx*)	1	0	0	0
Guerneuk (*Litocranius walleri*)	5	0	0	0
Giraffe (*Giraffa camelopardalis*)	7	0	3	3
Ovine (*Ovis aries*)	641	48	17	65
Thompson gazelle (*Gazella thompsoni*)	1	0	0	0
Water Buck (*Kobus ellipsipyrmnus*)	5	0	0	0
Warthog (*Phaecochoerus africanus*)	44	0	0	0
Zebra (*Equus grevyi*)	3	0	0	0
Total	3,250	163 (5.2%)	126 (4.0%)	289 (9.2%)

clinical materials or following virus isolation (Table 2). Where possible, RVF virus sequence data were obtained directly from the clinical specimens to reduce potential nucleotide variability introduced during virus isolation. We successfully obtained complete S, M, and L segment genome sequences for 27 of the specimens, with an additional 4 specimens yielding complete S segment genome sequences only (85 total segments). Typically, complete genome sequencing was successful with total RNA extracted directly from clinical specimens with RVF virus-specific qRT-PCR cycle threshold (C_T) values of less than ~30.0, which corresponds to calculated infectious virus titers of approximately 10 to 100 PFU/ml. The 31 virus specimens yielding complete RNA segment genome data were collected during a period of 6 months spanning the entire known epizootic period from early December 2006 through May 2007. Of these, 25 were collected from cattle, 3 from sheep, 2 from goats, and 1 from a buffalo, and they originated from throughout the affected regions of Kenya (Fig. 1, Table 2). Similarly to our previous work reporting the complete genome sequence data of 33 diverse RVF virus strains (6), little variation in the overall nucleotide lengths of the S, M, and L segments was found among the 2006-2007 viruses, with 1,690 to 1,691, 3,885, and 6,404 lengths obtained for the S, M, and L segments, respectively. Overall, the pairwise percent nucleotide identity differences between viruses present during the 2006-2007 epizootic were low, with 1.5, 1.6, and 1.1% found on the S, M, and L segments, respectively. Interestingly, these percent identity differences were larger than those found during previous large epizootic-epidemics in Egypt (~0.2%; 1977-1979) and Mauritania (~0.2%; 1987) (6).

Both maximum-likelihood and Bayesian-based (BEAST) phylogenetic analyses of these virus sequences demonstrated well-supported evidence of the presence of two main RVF virus lineages (Kenya-1 and Kenya-2) circulating during the 2006-2007 epizootic (Fig. 3 to 5). The finding of multiple virus lineages circulating concurrently within this epizootic is in contrast to findings for the 1977-1979 Egyptian and 1987 Mauritania RVF virus epizootics/epidemics, where only single lineages are apparent (Fig. 3 to 5). Twenty-five viruses formed a monophyletic Kenya-1 lineage with 100% posterior support. An internal sublineage (Kenya-1a; 100% posterior support) was formed within the Kenya-1 lineage by five viruses. In addition to the predominant Kenya-1 lineage, a separate and distinct lineage (Kenya-2) was revealed that contained a total of six viruses. Clear evidence of a recent RNA segment reassortment event between Kenya-1a and Kenya-2 lineages was found. RVF virus #0608 was found to have S and L segments firmly placed within the Kenya-1a lineage, but the M segment was firmly within the Kenya-2 lineage (Fig. 3 to 5), consistently with #0608 representing an M segment reassortant. Together these results indicate the presence of multiple virus genotypes during epizootics/epidemics within the east African geographic area of endemicity and that RNA segment reassortment (genetic shift) can contribute to RVF virus evolution.

Molecular evolutionary rates, selection of molecular clock/tree coalescent models, and TMRCA. Following the successful generation and alignment of each complete segment data set, multiple Bayesian (BEAST) MCMC runs were completed with strict, relaxed uncorrelated exponential, or relaxed uncorrelated log-normal molecular clock parameters, as well as population size coalescent parameters of either constant population size, exponential growth, or logarithmic growth. Both relaxed clock models allow for the simultaneous calculation of molecular clock rate data along individual phylogenic lineages and allow for the lineage-dependent flexibility of estimated molecular clock evolutionary rates. A comparison of models revealed that both relaxed uncorrelated exponential and logarithmic molecular clock models were highly favored for the S, M, and L segments over a strict molecular clock model, as indicated by log-normal Bayes factors of ~22, 20, and 25, respectively. Given the substantial preference for relaxed molecular clock models, all subsequent in-depth Bayesian analyses utilized the relaxed uncorrelated logarithmic clock model.

Using these relaxed-model parameters, the overall molecular evolutionary rate (nucleotide substitutions/site/year) of the entire data set was in agreement with previously reported rates (6). For each segment, the overall mean rate and 95% HPD interval for each segment was the following: S, 3.9×10^{-4} (2.4×10^{-4} to 5.5×10^{-4}); M, 3.6×10^{-4} (2.6×10^{-4} to 4.6×10^{-4}); and L, 2.8×10^{-4} (1.8×10^{-4} to 3.9×10^{-4}). The more complex relaxed log-normal clock implemented in these analyses allowed for the estimation of the molecular evolutionary

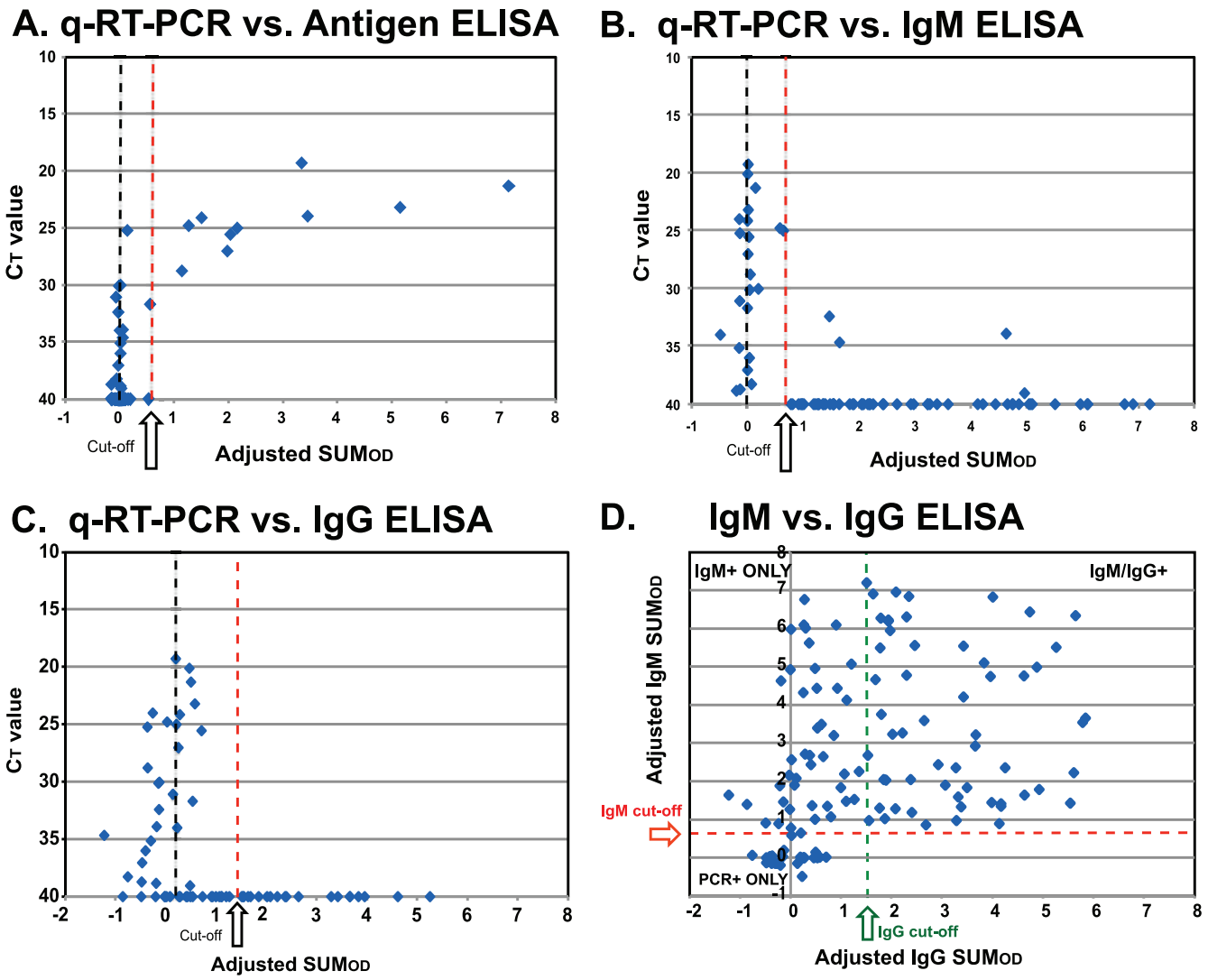

FIG. 2. RVF virus diagnostic assay performance. Results of serologic testing are reported as the adjusted SUM_{OD}, which was defined as the cumulative sum of the optical densities of each specimen dilution minus the background absorbance of uninfected control Vero E6 cells. (A) Pairwise comparison of the qRT-PCR C_T values (*y* axis) and RVF antigen capture ELISA adjusted SUM_{OD} values (*x* axis). qRT-PCR C_T values of less than 40 were considered positive. The cutoff SUM_{OD} value for the RVF antigen capture ELISA was conservatively set at >0.45 and is indicated by the dashed red line and arrow. (B) Pairwise comparison of the qRT-PCR C_T values (*y* axis) and anti-RVF virus IgM ELISA adjusted SUM_{OD} values (*x* axis). qRT-PCR C_T values of less than 40 were considered positive. The cutoff SUM_{OD} value for the anti-RVF virus specific IgM ELISA was conservatively set at >0.75 and is indicated by the dashed red line and arrow. Note the marked reduction in qRT-PCR-positive (n = 3) specimens after individual animals became seropositive for anti-RVF virus-specific IgM. (C) Pairwise comparison of the qRT-PCR C_T values (*y* axis) and anti-RVF virus IgG ELISA adjusted SUM_{OD} values (*x* axis). qRT-PCR C_T values of less than 40 were considered positive. The cutoff SUM_{OD} value for the anti-RVF virus specific IgG ELISA was conservatively set at >1.50 and is indicated by the dashed red line and arrow. (D) Pairwise comparison of anti-RVF virus IgM ELISA adjusted SUM_{OD} values (*y* axis) and anti-RVF virus IgG ELISA adjusted SUM_{OD} values (*x* axis) of all RVF virus-positive specimens (recent and past). The cutoff values of the IgM and IgG ELISAs are indicated by the red horizontal dashed line and green vertical dashed line, respectively. The resulting chart is divided into quadrants, with the upper left quadrant indicating specimens that were positive only for IgM serology, the upper right quadrant indicating specimens that were both IgM and IgG positive, and the lower left quadrant indicating specimens positive by qRT-PCR only.

rates specifically for the 2006-2007 RVF virus lineages separately from all other viruses. Interestingly, the mean rates of the S, M, and L segments were approximately two- to fourfold higher than the overall molecular evolutionary rate of the entire RVF virus genome collection, consistently with the expansion of the effective population size and increased virus activity and nucleotide diversity during the outbreak. Mean molecular evolution rates for the Kenya-1 lineage were 7.6×10^{-4}, 4.0×10^{-4}, and 4.3×10^{-4} nucleotide substitutions/site/year for the S, M, and L segments, respectively. Likewise, the calculated rates for the Kenya-2 lineage were increased, with mean values of 9.8×10^{-4}, 4.3×10^{-4}, and 3.0×10^{-4} for the S, M, and L segments, respectively.

The most recent common ancestor of any collection of genomes is defined, in a broad sense, as the most recently occurring ancestral genotype that is the progenitor of that group.

TABLE 2. Summary of RVF virus specimens sequenced

Specimen identity no.	Species: specimen type	Administrative district of origin	Date collected (day/mo/yr)	Passage history[a] of segment:		
				S	M	L
2007000080	Bovine: serum	Maragua	12 Jan 07	*	*	*
2007000094	Bovine: serum	Garissa	12 Jan 07	*	E6 + 1	E6 + 1
2007000222	Bovine: serum	Maragua	16 Jan 07	*	*	*
2007000223	Bovine: serum	Maragua	16 Jan 07	*	*	*
2007000224	Bovine: serum	Maragua	16 Jan 07	*	E6 + 1	E6 + 1
2007000225	Bovine: serum	Maragua	16 Jan 07	*	*	*
2007000226	Bovine: serum	Maragua	16 Jan 07	*	–	–
2007000473	Ovine: liver	Kajaido	26 Jan 07	*	*	*
2007000608	Bovine: serum	Meru South	29 Jan 07	*	*	*
2007000611	Bovine: serum	Meru South	29 Jan 07	*	*	*
2007000618	Bovine: serum	Meru South	29 Jan 07	*	E6 + 1	E6 + 1
2007000665	Bovine: serum	Nyeri	26 Jan 07	*	–	–
2007001107	Bovine: liver	Thika	25 Jan 07	*	*	*
2007001292	Bovine: liver	Meru South	31 Jan 07	*	*	*
2007001443	Bovine: liver	Nakuru	31 Jan 07	*	*	*
2007001564	Bovine: serum	Muranga	29 Jan 07	*	E6 + 1	E6 + 1
2007001602	Bovine: liver	Mombassa	30 Jan 07	*	E6 + 1	E6 + 1
2007001800	Bovine: blood	Nairobi	26 Jan 07	*	–	–
2007001809	Caprine: serum	Garissa	01 Dec 06	*	*	*
2007001811	Caprine: liver	Garissa	01 Dec 06	*	*	*
2007002059	Ovine: liver	Nairobi	07 Feb 07	*	–	–
2007002060	Bovine: blood	Nairobi	31 Jan 07	*	*	*
2007002444	Bovine: blood	Meru Central	05 Feb 07	*	*	*
2007002445	Bovine: blood	Meru Central	05 Feb 07	*	*	*
2007002476	Bovine: liver	Nakuru	21 Feb 07	*	*	*
2007002482	Bovine: liver	Thika	21 Feb 07	*	*	*
2007002820	Buffalo: serum	Garissa	09 Feb 07	E6 + 1	E6 + 1	E6 + 1
2007003081	Bovine: serum	Mbeere	27 Feb 07	*	*	*
2007003644	Ovine: serum	Baringo	07 Feb 07	E6 + 1	E6 + 1	E6 + 1
2007004193	Bovine: liver	Nairobi	23 Apr 07	*	*	*
2007004194	Bovine: blood	Kiambu	14 May 07	*	*	*

[a] The complete RNA segment genome sequence was derived either directly from clinical materials (i.e., serum, whole blood, or liver tissue; indicated by an asterisk) or after virus isolation in Vero E6 cells (E6 + 1). A dash indicates that no sequence data was obtained.

Consistently with previous analyses (6), the overall common ancestry of each of the three (S, M, and L) expanded complete segment datasets was found to be relatively recent, with the TMRCA of all samples coalescing toward values approximately 87 to 112 years before the present (Fig. 3 to 5).

Insights into RVF virus 2006-2007 epizootic ecology and shared ancestry with 1997-1998 East African outbreak. All 31 viruses identified during the 2006-2007 outbreak were phylogenetically grouped into a common Kenyan RVF virus lineage (Fig. 3 to 5). Interestingly, these 31 viruses were most closely related to a representative RVF virus (#0523) detected in Kenya during the previous large East African outbreak that occurred during 1997-1998 (Fig. 3 to 5). The RVF virus lineages involved during both of these recent large outbreaks likely have been present in Kenya since at least the early 1980s, as evidenced by the formation of a single monophyletic group (100% posterior support) containing the S, M, and L segments of these viruses and an RVF virus (strain 21445) collected in 1983 (Fig. 3 to 5). In addition, the Saudi Arabian outbreak viruses of the large 2000 outbreak share a common ancestor with this Kenyan lineage, confirming earlier genetic data that indicated the recent introduction of virus into the Arabian Peninsula (6). Historically, additional RVF virus lineages have been present in Kenya, as evidenced by the presence of the 1965 Kenyan isolate (Kenya56) that shared a common ancestor with viruses from Zimbabwe (763/70) and South Africa (SA75). This lineage was not detected in either the 1997-1998 or 2006-2007 outbreak.

While the shared evolutionary history of the 1997-1998 and 2007 RVF outbreak viruses is apparent on the basis of phylogeny, more detailed Bayesian analyses were completed to more fully characterize this relationship. These analyses indicated that the TMRCA of the 2006-2007 Kenya-1 and Kenya-2 lineages likely occurred shortly before or during the previous 1997-1998 outbreak (Fig. 3 to 5). The mean and 95% HPD interval (in parentheses) TMRCA estimates for the S, M, and L segments of the 2006-2007 RVF viruses were 9.5 (4.5 to 16 years), 18.6 (13.1 to 24.4 years), and 16.5 years (10.0 to 22.1 years). Taken together, these data suggest that the progenitor virus of these two lineages of 2006-2007 outbreak RVF viruses was present sometime during the mid- to late 1990s. This finding was unexpected and adds substantial evidence for the endemic stability of specific RVF virus genotypes in the Kenyan ecosystem and clearly demonstrates the ability of a single RVF virus lineage to contribute to multiple periodic outbreak events over relatively long time periods.

Evidence of interoutbreak RVF virus expansion and ongoing virus lineage evolution since the 1997-1998 epizootic/epidemic. MSNs also demonstrated clear evidence of two main RVF virus lineages (Fig. 6). Surprisingly, each lineage (Kenya-1 and Kenya-2) was more closely related to the 1997-1998 Kenyan outbreak prototype than they were to each other (Fig. 6). The

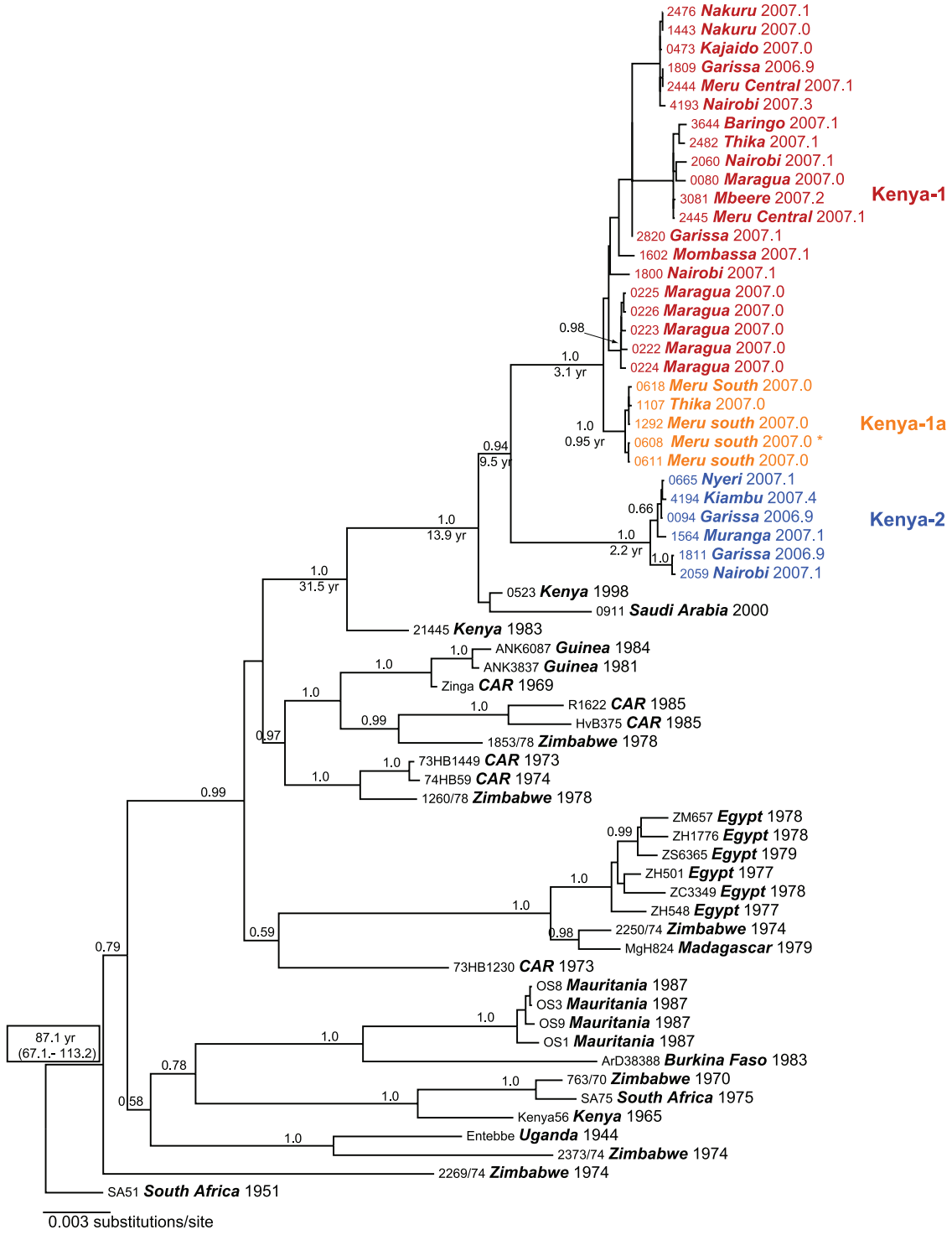

FIG. 3. RVF virus S segment maximum a posteriori clade credibility tree generated using BEAST-v1.4.7/Tree annotator/Fig Tree-v1.1.2. The combined MCMC chain length was 9.0×10^7 steps; 2.25×10^7 steps (25%) were removed as the burn in. Posterior support values (HPD) are indicated as integers (i.e., 100% support = 1.0) above each node. The calculated mean TMRCAs are indicated below each respective node and are enumerated as years before the collection date of the last outbreak specimen (May 2007). Note that 31 individual complete RVF virus S segments were obtained. The main Kenya-1 lineage is indicated in red, with the sublineage Kenya-1a in orange and the separate Kenya-2 lineage depicted in blue.

majority of haplotypes were found within lineage Kenya-1 and exhibited a star-like pattern, indicating possible recent demographic or spatial expansion, whereas lineage Kenya-2 was represented by only four haplotypes (Fig. 6). Consistently with the phylogenetic analyses (Fig. 3 to 5), a possible M segment reassortment event was observed (Fig. 6).

Based on the identification of two distinct lineages in the outbreak, mismatch distributions and subsequent tests for pop-

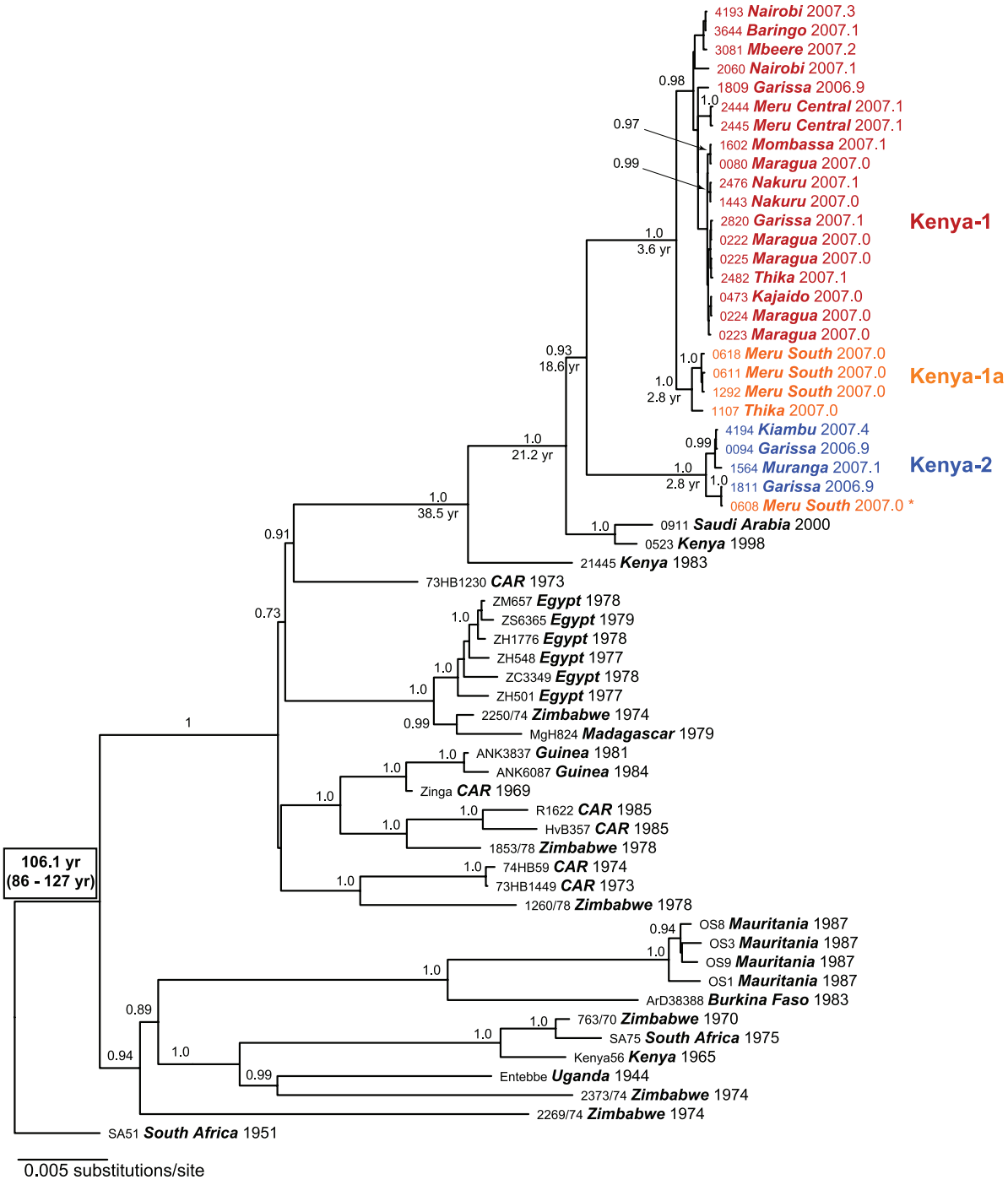

FIG. 4. RVF virus M segment maximum a posteriori clade credibility tree generated using BEAST-v1.4.7/Tree annotator/Fig Tree-v1.1.2. The combined MCMC chain length was 9.0×10^7 steps; 2.25×10^7 steps (25%) were removed as the burn in. Posterior support values (HPD) are indicated as integers (i.e., 100% support = 1.0) above each node. The calculated mean TMRCAs are indicated below each respective node and are enumerated as years before the collection date of the last outbreak specimen (May 2007). Note that 27 individual complete RVF virus M segments were obtained. The main Kenya-1 lineage is indicated in red, with the sublineage Kenya-1a in orange and the separate Kenya-2 lineage depicted in blue.

ulation expansion were conducted on each lineage independently and for each virus genome segment. Mismatch distribution analyses of the S, M, and L segments of lineage Kenya-1 provided strong evidence that an increase in virus population size and spatial distribution had occurred (Fig. 7A, Table 3). However, no mismatch distributions for lineage Kenya-2 were significant, likely due to the small numbers of virus haplotypes ($n = 4$) contained within the lineage (Fig. 7).

Further analyses utilizing the Tajima's D test (53) were completed and were consistent with significant evidence of either

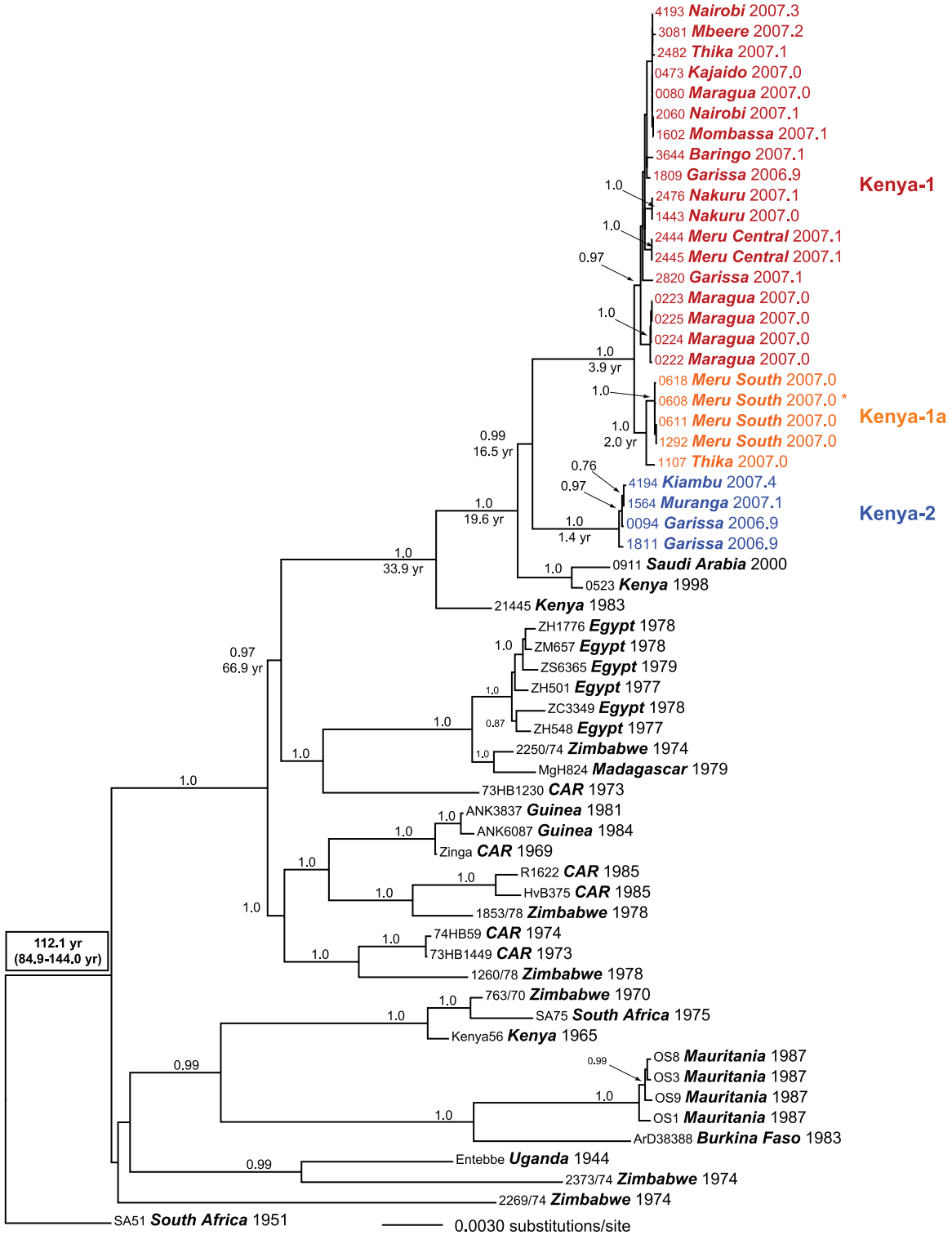

FIG. 5. RVF virus L segment maximum a posteriori clade credibility tree generated using BEAST-v1.4.7/Tree annotator/Fig Tree-v1.1.2. The combined MCMC chain length was 9.0×10^7 steps; 2.25×10^7 steps (25%) were removed as the burn in. Posterior support values (HPD) are indicated as integers (i.e., 100% support = 1.0) above each node. The calculated mean TMRCAs are indicated below each respective node and are enumerated as years before the collection date of the last outbreak specimen (May 2007). Note that 27 individual complete RVF virus L segments were obtained. The main Kenya-1 lineage is indicated in red, with the sublineage Kenya-1a in orange and the separate Kenya-2 lineage depicted in blue.

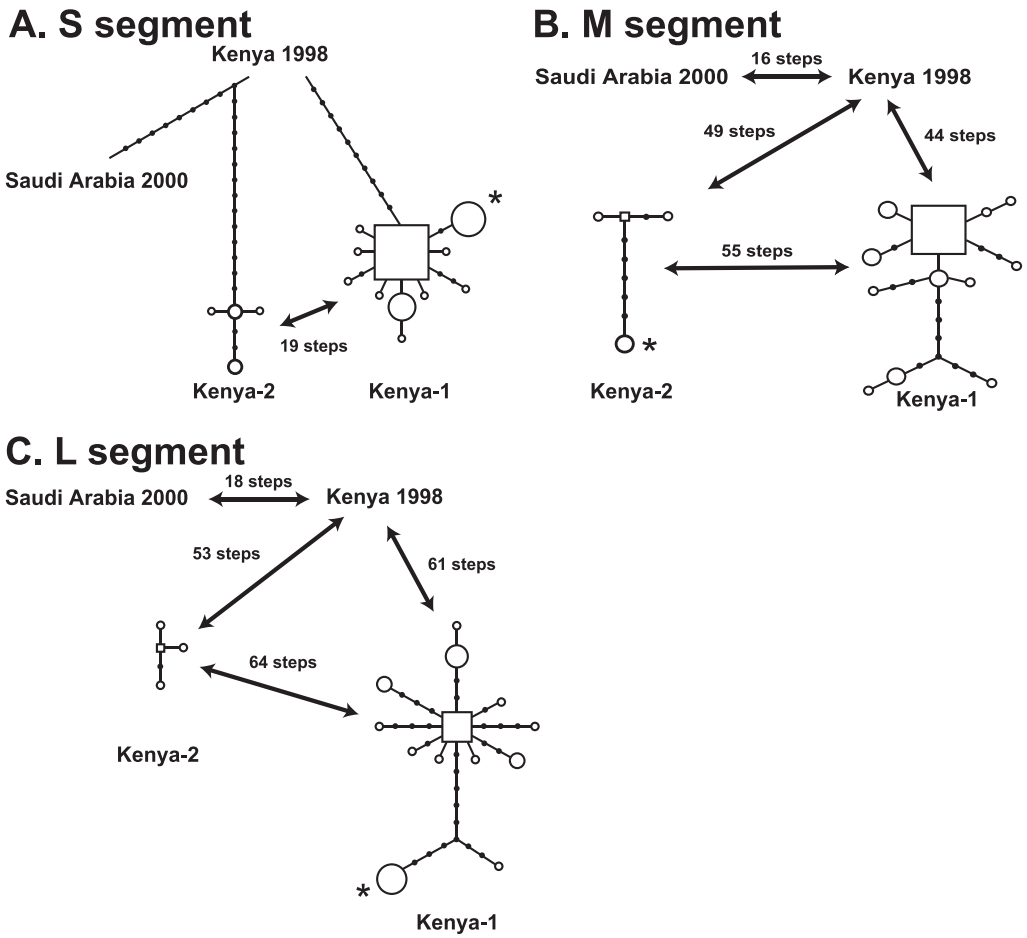

FIG. 6. MSNs visually describing discrete genetic distances between unique haplotypes for the S, M, and L RVF virus genome segments. Each node represents one nucleotide difference between extant (open circle) or inferred (filled black circle) haplotypes. Proportionally larger open circles or squares represent the relative number of extant haplotypes represented in the network. Note the greater distance measured in nucleotide changes (steps) between the Kenya-1 and Kenya-2 lineages than that with the prototype Kenyan 1997-1998 RVF virus strain. Also note the star-like phylogeny of the Kenya-1 lineage, indicating the potential of recent increases in virus population size or geographic range. An asterisk on each MSN indicates the relative position of the putative M segment reassortant virus (#0608).

population expansion or potential purifying selection for the S and M segments of the Kenya-1 lineage (Table 3). Additionally, Fu's Fs test (20), which is particularly sensitive to population expansion, demonstrated that the Kenya-1 lineage S segment recently had undergone significant expansion; however, values based on the M and L segments were not significant (Table 3). This finding was unexpected and likely due to the intrinsic nature of Fu's Fs test, which exhibits atypical decreases in power with increasing sample size or numbers of segregating sites (42). No significant results were observed for lineage Kenya-2 based on either test. Taken together, these analyses indicate that since the recent divergence of the Kenya-1 and Kenya-2 lineages, the Kenya-1 lineage has experienced significant expansion while the Kenya-2 lineage likely has not.

Among the 2006-2007 RVF viruses, no correlation between genetic diversity and the time of specimen collection was found during the outbreak period (data not shown). Although this lack of association could be consistent with a young and/or rapidly expanding population, it is likely that the relatively short duration of the outbreak and sampling period obscured any detectable relationship. Similarly, no strong correlation of genetic and geographic distance was detected for the outbreak samples, although a weak signature of isolation by distance was observed for the lineage Kenya-1 S segment samples [$r(AB)$ (an internal measure of correlation) = 0.300; $P < 0.05$] (see Fig. S1 in the supplemental material).

Using a population genetics-based approach, the timing of the observed population expansion for lineage Kenya-1 was calculated using an overall mutation rate of 2.9×10^{-4} nucleotide substitutions/site/year, as determined previously (6). Given a τ value of 2.03 for the S segment, the expansion event would have occurred 2.05 years prior to the detection of the most recent Kenyan RVF virus outbreak. Estimates of expansion based on the M and L segments (τ values of 8.5 and 13.594, respectively) placed the time of expansion slightly earlier, at 3.77 and 3.66 years prior to the 2006/2007 outbreak, respectively. These population genetics-based results were highly congruent with TMRCA data obtained independently by rigorous Bayesian estimation (BEAST) of the timing of the evolutionary origins and the most recent common ancestor of the Kenya-1 lineage (Fig. 2 to 4). The mean and 95% HPD interval (in parentheses) estimates of the TMRCA for the S,

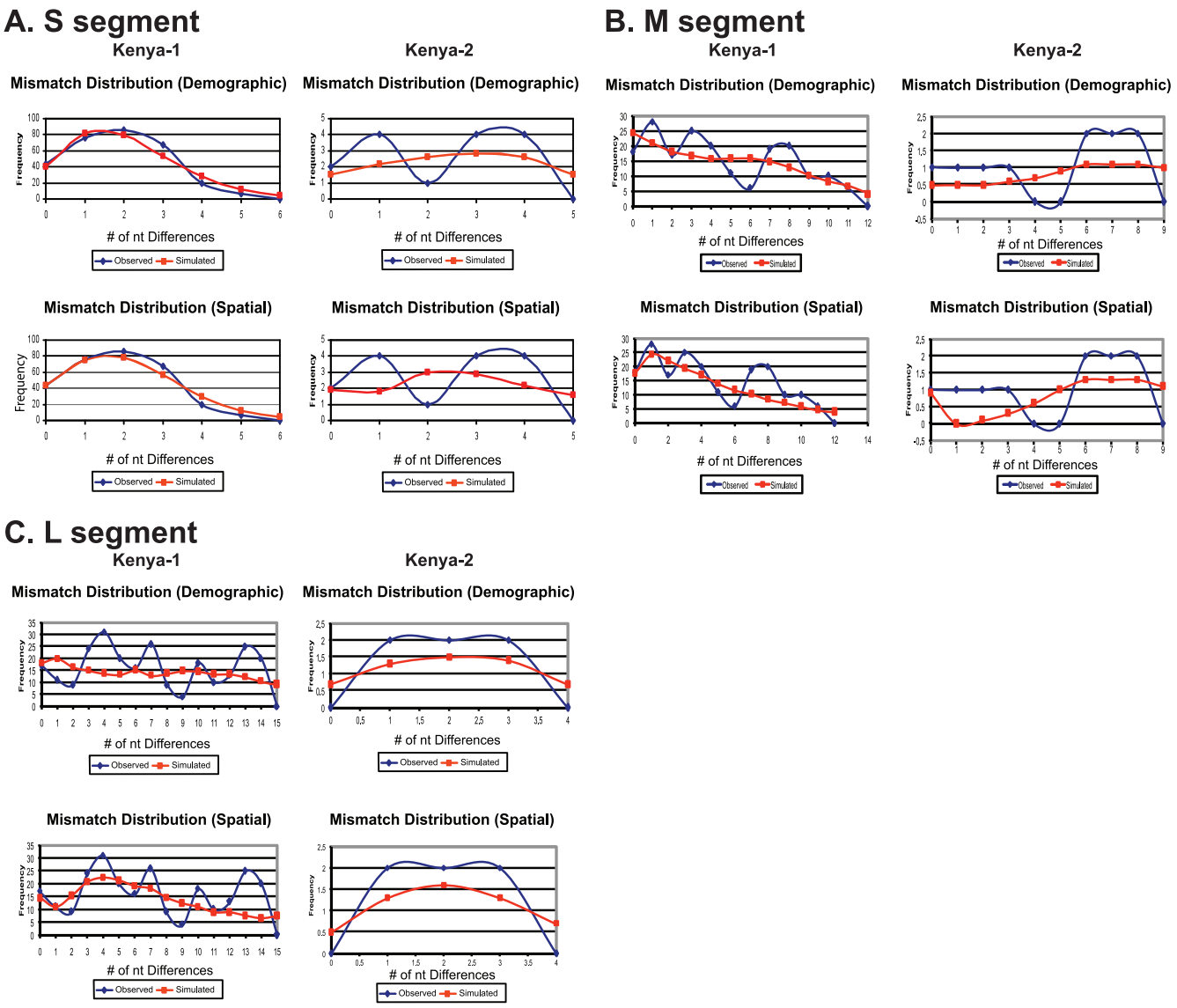

FIG. 7. Mismatch distributions of the Kenya-1 and Kenya-2 lineage S, M, and L RVF virus genome segments. In each panel, the mismatch distributions of the Kenya-1 lineage are depicted on the left, with the Kenya-2 mismatch distributions depicted on the right. The actual observed frequencies of nucleotide (nt) substitutions between unique haplotypes are depicted in blue with diamond data markers. Simulated data of recent exponential population demographic expansion are depicted in red with square data markers. Analyses of the S segment were clearly unimodal for lineage Kenya-1, allowing for the rejection of the null hypothesis of stable population size and spatial expansion ($P = 0.57$ and 0.61, respectively) and providing evidence that an increase in virus population size and spatial distribution had occurred. Mismatch distributions for lineage Kenya-1 based on the M and L segments appeared to be multimodal, but no significant differences were found between the observed data and that simulated under a model of sudden expansion (M, $P = 0.94$ and 0.89; L, $P = 0.70$ and 0.62). Based on these results, the evidence of recent exponential population expansion prior to the 2006-2007 outbreak could not be ruled out for the S, M, and L RVF virus genome segments of the Kenya-1 lineage.

M, and L segments of the Kenya-1 lineage were 3.1 (1.2 to 5.5), 3.6 (1.9 to 5.6), and 3.9 (2.0 to 6.1) years before the 2006/2007 outbreak. Taken together, these results suggest that an undetected and significant demographic and spatial expansion of RVF virus occurred during the intervening years between the 1997-1998 and 2006-2007 outbreaks.

DISCUSSION

The data presented here provide, for the first time, a comprehensive examination of complete virus genome sequence distribution and evolution during an outbreak and a description of the dynamics and development of a widespread epizootic among livestock in an area in which RVF virus activity is endemic. The results of diagnostic testing revealed approximately similar levels of recent RVF virus infection among the cattle, sheep, goats, and camels sampled during the outbreak period, indicating their importance in the development of the RVF virus epizootic (Table 1). The high impact of RVF virus infection both directly (mortality/morbidity) and indirectly (economic/nutritional) on the human and animal population highlights the far-reaching effects of extensive epizootics.

TABLE 3. RVF virus population genetics analyses

Lineage and segment	Result by[a]:		
	Fu's Fs	Tajima's D	HRI
Kenya-1			
S	−5.33409*	−1.71095*	0.04347
M	−0.77503	−2.22568*	0.02044
L	−1.48675	−1.24869	0.02661
Kenya-2			
S	−0.27174	0.56168	0.16889
M	−0.66392	−0.82943	0.09000
L	−1.87180	−0.78012	0.22222

[a] An asterisk indicates significance at $P = 0.05$. HRI, Harpending's raggedness index.

The importance and utility of a combined approach using both molecular (qRT-PCR) and classical serologic techniques (IgM and IgG) cannot be underestimated (Fig. 2). During this large widespread outbreak, the majority of acute infections were identified by anti-RVF virus-specific IgM alone, with a relatively small proportion identified exclusively by qRT-PCR (Fig. 2B and D). While the real-time and high-throughput nature of qRT-PCR techniques are advantageous in certain circumstances over classical serology, the data presented here clearly demonstrate that diagnostic efforts for RVF virus infection must include a comprehensive approach for the detection of both virus/RNA and IgM/IgG antibodies (Fig. 2). Due to the early induction of humoral immune responses, a substantial proportion of infected animals potentially are negative for the presence of virus RNA by the time infected herds are recognized and samples are taken. These data would advise against the sole reliance on qRT-PCR techniques for the early identification of nascent outbreak activity in either previously unaffected areas or areas in which the virus is endemic following the accidental or intentional release of this significant public health and veterinary pathogen.

The generation of a large number of complete virus genomes spanning the entire geographic and temporal distribution of virus activity during the 2006-2007 RVF virus epizootic/epidemic allowed us to more closely examine overall intraoutbreak genomics than was possible in previous studies, which were limited by the small numbers of viruses or genome regions analyzed (6, 14, 38, 46, 48). In contrast with previous reports (6, 48), which sought to examine the phylogenetic relationships of the Egyptian 1977-1979/Mauritania 1987 and Saudi Arabia 2000 outbreaks, the 2006-2007 data contained clear evidence of multiple virus lineages actively circulating during the outbreak period (Fig. 3 to 5). This contrast likely reflects differences in the initiating events of each respective outbreak. While the 2006-2007 epizootic/epidemic occurred within an area in which the virus is historically endemic, the Egyptian, Mauritanian, and Saudi Arabian genomic data likely represents the largely virgin-soil nature of these outbreaks, with single or limited introductions of virus genotypes into these areas.

However, the genomic diversity observed in the 2006-2007 outbreak still was much less than that observed among virus isolates collected in Zimbabwe in the 1970s during a period of either endemic or localized epizootic activity (52). During this time period, virus isolates collected within a relatively small geographic area (~170-km radius of the capitol city Harare) were found within several RVF virus lineages containing representatives from throughout eastern, western, and central Africa (Fig. 3 to 5). Although Zimbabwe and Kenya both have historically been areas in which RVF virus activity is endemic, interesting differences in the ecologic maintenance of overall genomic diversity may exist between each location.

The clear ancestral relationship of the viruses detected in 2006-2007 with that of a previous RVF virus isolated 25 years previously in Kenya in 1983 from an *Aedes mcintoshii* mosquito was surprising and illustrates that the endemic maintenance of RVF virus in the Kenyan ecosystem can result from the continued presence of a specific RVF virus lineage (Fig. 3 to 5). Since that time, reports of significant RVF virus activity/outbreaks have occurred a limited number of times, including the large 1997-1998 epizootic/epidemic (8, 61). The direct ancestry of the 2006-2007 outbreak viruses from the viruses of the previous 1997-1998 outbreak was evident on the basis of phylogeny, with the most probable TMRCAs of all 2006-2007 viruses estimated to be either immediately prior to or during the 1997-1998 outbreak (Fig. 3 to 5). This finding demonstrates the potential public health and veterinary impact of the reemergence of a single RVF virus lineage during at least a 10-year period resulting in large epizootic/epidemic events.

We provide here the first direct genomic data confirming ongoing RVF virus evolution and activity during the interepidemic period. While widespread and explosive RVF virus outbreaks are hallmarks of the virus life cycle, evidence of a cryptic enzootic cycle of transmission can be found among seroprevalence survey data of wildlife and human populations throughout Kenya (18, 23, 27), with more direct data derived by virus isolation and transmission studies in vector populations during interepidemic periods (30, 32, 33). Surprisingly, both Bayesian phylogenetic and population genetics-based estimates of the ancestry and population dynamics of the Kenya-1 and Kenya-2 lineages revealed an estimated time period of RVF virus activity and population expansion approximately 2 to 4 years prior to the 2006-2007 epizootic/epidemic (Fig. 3 to 5 and 7).

To determine if the proper ecological conditions existed for this predicted increase in activity during this time period, the results of normalized vegetative difference imaging (NDVI) and risk analyses of RVF virus activity (http://www.geis.fhp.osd.mil/GEIS/SurveillanceActivities/RVFWeb/indexRVF.asp) were examined. During the time period for which analyses were available (January 2000 to January 2008), there were two periods of greatly increased potential for RVF virus activity in northeastern Saharan Africa focused along the border regions of Kenya, Ethiopia, and Somalia during the winter months of 2004-2005 and 2002-2003, or approximately 2 to 4 years prior to the 2006-2007 outbreak. This environmental data, coupled with our genomic analyses, which revealed a recent population expansion event, and the TMRCA estimates of the 2006-2007 viruses strongly suggest that significant RVF virus activity occurred in the region undetected during this time period. No published reports of RVF virus infection could be found regarding livestock or humans in the region during these time periods. It is possible that limited transmission during this time period would have been below the threshold of detection by either public health or veterinary authorities. Clearly, the development and timing

of epizootic/epidemic events are complex, likely requiring the confluence of multiple factors, such as the availability of susceptible hosts, the presence of transovarially infected vectors, and environmental conditions conducive to virus propagation and dissemination.

Interestingly, further comparisons of the Kenya-1 and Kenya-2 lineages showed contrasting patterns of virus evolution between these two closely related groups. While significant evidence of expansion of the Kenya-1 lineage was demonstrated (Fig. 7, Table 3), the Kenya-2 lineage did not possess the same signatures of expansion despite the cocirculation of both lineages over the same time period. This may be due simply to the small sample size of the Kenya-2 lineage, but more likely it reflects the less prevalent nature of this virus lineage throughout the Kenyan ecosystem.

Consistently with previous laboratory and field reports (3, 6, 45), the detection of a reassortant virus containing both Kenya-1 and Kenya-2 genome segments indicates that interactions and the exchange of genetic material between each lineage via superinfection are possible. These data, taken together, suggest that although RVF virus exists as a single serotype throughout its geographic range (47), potentially biologically important differences in reproductive fitness exist among virus lineages and subpopulations in their natural environment.

The lack of an isolation by distance signature in the data from this outbreak suggests that the relative impact of the mosquito-borne dispersal of virus during the outbreak could have been significant, as some mosquito species potentially can travel over distances greater than 150 km (25). However, it is more likely that these viruses were already distributed throughout the country as a result of earlier epizootics/epidemics. Taken together, these population genetics-based findings support a hypothesis of an apparent shift of RVF virus activity primarily due to alterations in overall rainfall patterns and the eruption of virus activity from local habitats rather than direct animal-to-animal or wave-like spread throughout the country.

The findings of ongoing RVF virus activity and evolution during intraepizootic/epidemic periods are significant and have implications for both the design of enhanced surveillance programs in regions throughout Africa in which the virus is endemic and future studies of RVF virus ecology. Our findings of RVF virus activity and population expansion without accompanying reports of human or livestock illness suggests that appropriate disease surveillance programs, coupled with the predictive power of NDVI, could identify areas with enhanced RVF virus activity risk and increase the likelihood of detecting otherwise cryptic RVF virus activity (7, 57). Additionally, the early warning potential of NDVI analyses could allow for a window of opportunity for the prophylactic deployment of safe and effective RVF virus vaccines to target either areas at greatest risk or highly valuable livestock animals in areas in which the virus is endemic.

The recent introduction of another significant vector-borne veterinary pathogen (bluetongue virus serotype 8) into northern Europe illustrates the difficulties inherent in control efforts for arthropod-borne pathogens and their dramatic impact on international livestock trade (16, 17, 58). A similar situation could be envisaged for RVF virus based on the evidence of the widespread geographic movement of RVF virus (6) over its evolutionary history. These data suggest that after introduction into previously unaffected regions, the rapid identification and control of a nascent RVF virus epizootic/epidemic will be critical to prevent widespread dissemination. Central to these future RVF virus control efforts are integrated diagnostic approaches similar to those described here and the close coordination of public health, entomologic, and veterinary authorities for the control of this significant health threat.

ACKNOWLEDGMENTS

We thank Phillip Nyaga, Robert Breiman, Kariuki Njenga, and Alan Hightower for their support in facilitating the international collaborative effort reported here. We also thank Gary Goolsby for his helpful assistance during the deployment of the CDC outbreak team and Andrew Rambaut for his helpful comments regarding the Bayesian phylogenetic techniques reported here. We thank Karl Kincade and Craig Manning for assistance with data mapping. B.H.B. thanks N. James MacLachlan (UCD SVM) for his steadfast support and encouragement.

The Office of Foreign Disaster Assistance, USAID, provided generous support for the equipping of the RVF virus diagnostic laboratory in Kabete. B.H.B. was supported by the dual-degree DVM/Ph.D. Veterinary Scientist Training program (VSTP) and the Students Training in Advanced Research program of the University of California Davis School of Veterinary Medicine and the Oak Ridge Institute of Science Education (ORISE).

The findings reported here are those of the authors and do not necessarily represent those of the Centers for Disease Control and Prevention or the government of the Republic of Kenya.

REFERENCES

1. **Anonymous.** 2007. Outbreaks of Rift Valley fever in Kenya, Somalia and United Republic of Tanzania, December 2006-April 2007. Wkly. Epidemiol. Rec. **82**:169–178.
2. **Anyamba, A., J. P. Chretien, J. Small, C. J. Tucker, and K. J. Linthicum.** 2006. Developing global climate anomalies suggest potential disease risks for 2006-2007. Int. J. Health Geogr. **5:**60.
3. **Beaty, B. J., E. J. Rozhon, P. Gensemer, and D. H. Bishop.** 1981. Formation of reassortant bunyaviruses in dually infected mosquitoes. Virology **111:**662–665.
4. **Bird, B. H., C. G. Albarino, and S. T. Nichol.** 2007. Rift Valley fever virus lacking NSm proteins retains high virulence in vivo and may provide a model of human delayed onset neurologic disease. Virology **362:**10–15.
5. **Bird, B. H., D. A. Bawiec, T. G. Ksiazek, T. R. Shoemaker, and S. T. Nichol.** 2007. Highly sensitive and broadly reactive quantitative reverse transcription-PCR assay for high-throughput detection of Rift Valley fever virus. J. Clin. Microbiol. **45:**3506–3513.
6. **Bird, B. H., M. L. Khristova, P. E. Rollin, T. G. Ksiazek, and S. T. Nichol.** 2007. Complete genome analysis of 33 ecologically and biologically diverse Rift Valley fever virus strains reveals widespread virus movement and low genetic diversity due to recent common ancestry. J. Virol. **81:**2805–2816.
7. **Bowen, M. D., S. G. Trappier, A. J. Sanchez, R. F. Meyer, C. S. Goldsmith, S. R. Zaki, L. M. Dunster, C. J. Peters, T. G. Ksiazek, and S. T. Nichol.** 2001. A reassortant bunyavirus isolated from acute hemorrhagic fever cases in Kenya and Somalia. Virology **291:**185–190.
8. **Centers for Disease Control and Prevention.** 1998. Rift Valley fever—East Africa 1997–1998. MMWR Morb. Mortal. Wkly. Rep. **47**:261–264.
9. **Centers for Disease Control and Prevention.** 2007. Rift Valley fever outbreak–Kenya, November 2006-January 2007. MMWR Morb. Mortal. Wkly. Rep. **56**:73–76.
10. **Clement, M., D. Posada, and K. A. Crandall.** 2000. TCS: a computer program to estimate gene genealogies. Mol. Ecol. **9:**1657–1659.
11. **Coetzer, J. A.** 1982. The pathology of Rift Valley fever. II. Lesions occurring in field cases in adult cattle, calves and aborted foetuses. Onderstepoort J. Vet. Res. **49:**11–17.
12. **Daubney, R., J. R. Hudson, and P. C. Garnham.** 1931. Enzootic hepatitis or Rift Valley fever. An undescribed virus disease of sheep cattle and man from East Africa. J. Pathol. Bacteriol. **34:**545–579.
13. **Drummond, A. J., and A. Rambaut.** 2007. BEAST: Bayesian evolutionary analysis by sampling trees. BMC Evol. Biol. **7:**214.
14. **Durand, J. P., M. Bouloy, L. Richecoeur, C. N. Peyrefitte, and H. Tolou.** 2003. Rift Valley fever virus infection among French troops in Chad. Emerg. Infect. Dis. **9:**751–752.
15. **Easterday, B. C., M. H. McGavran, J. R. Rooney, and L. C. Murphy.** 1962. The pathogenesis of Rift Valley fever in lambs. Am. J. Vet. Res. **23:**470–479.

16. **Enserink, M.** 2008. Animal disease. Exotic disease of farm animals tests Europe's responses. Science **319:**710–711.
17. **European Comission.** 2007. Commission regulation (EC) No. 1266/2007 of 26 October 2007 on implementing rules for Council Directive 2000/75/EC as regards the control, monitoring, surveillance and restrictions on movements of certain animals of susceptible species in relation to bluetongue, vol. L. Official Journal the European Union **283**:37–52.
18. **Evans, A., F. Gakuya, J. T. Paweska, M. Rostal, L. Akoolo, P. J. Van Vuren, T. Manyibe, J. M. Macharia, T. G. Ksiazek, D. R. Feikin, R. F. Breiman, and M. Kariuki Njenga.** 2008. Prevalence of antibodies against Rift Valley fever virus in Kenyan wildlife. Epidemiol. Infect. **136:**1261–1269.
19. **Excoffier, L., and S. Schneider.** 2005. Arlequin ver. 3.0: an integrated software package for population genetics analysis. Evol. Bioinformatics **2005:** 47–50.
20. **Fu, Y. X.** 1997. Statistical tests of neutrality of mutations against population growth, hitchhiking and background selection. Genetics **147:**915–925.
21. **Galtier, N., M. Gouy, and C. Gautier.** 1996. SEAVIEW and PHYLO_WIN: two graphic tools for sequence alignment and molecular phylogeny. Comput. Appl. Biosci. **12:**543–548.
22. **Gerrard, S. R., B. H. Bird, C. G. Albarino, and S. T. Nichol.** 2007. The NSm proteins of Rift Valley fever virus are dispensable for maturation, replication and infection. Virology **359:**459–465.
23. **Johnson, B. K., D. Ocheng, A. Gichogo, M. Okiro, D. Libondo, P. M. Tukei, M. Ho, M. Mugambi, G. L. Timms, and M. French.** 1983. Antibodies against haemorrhagic fever viruses in Kenya populations. Trans. R. Soc. Trop. Med. Hyg. **77:**731–733.
24. **Katoh, K., K. Kuma, T. Miyata, and H. Toh.** 2005. Improvement in the accuracy of multiple sequence alignment program MAFFT. Genome Inform. **16:**22–33.
25. **Kay, B. H., and R. A. Farrow.** 2000. Mosquito (Diptera: Culicidae) dispersal: implications for the epidemiology of Japanese and Murray Valley encephalitis viruses in Australia. J. Med. Entomol. **37:**797–801.
26. **Ksiazek, T. G., A. Jouan, J. M. Meegan, B. Le Guenno, M. L. Wilson, C. J. Peters, J. P. Digoutte, M. Guillaud, N. O. Merzoug, and E. M. Touray.** 1989. Rift Valley fever among domestic animals in the recent West African outbreak. Res. Virol. **140:**67–77.
27. **LaBeaud, A. D., Y. Ochiai, C. J. Peters, E. M. Muchiri, and C. H. King.** 2007. Spectrum of Rift Valley fever virus transmission in Kenya: insights from three distinct regions. Am. J. Trop. Med. Hyg. **76:**795–800.
28. **Le May, N., S. Dubaele, L. Proietti De Santis, A. Billecocq, M. Bouloy, and J. M. Egly.** 2004. TFIIH transcription factor, a target for the Rift Valley hemorrhagic fever virus. Cell **116:**541–550.
29. **Linthicum, K. J., A. Anyamba, C. J. Tucker, P. W. Kelley, M. F. Myers, and C. J. Peters.** 1999. Climate and satellite indicators to forecast Rift Valley fever epidemics in Kenya. Science **285:**397–400.
30. **Linthicum, K. J., C. L. Bailey, F. G. Davies, A. Kairo, and T. M. Logan.** 1988. The horizontal distribution of Aedes pupae and their subsequent adults within a flooded dambo in Kenya: implications for Rift Valley fever virus control. J. Am. Mosquito Control Assoc. **4:**551–554.
31. **Linthicum, K. J., C. L. Bailey, F. G. Davies, and C. J. Tucker.** 1987. Detection of Rift Valley fever viral activity in Kenya by satellite remote sensing imagery. Science **235:**1656–1659.
32. **Linthicum, K. J., F. G. Davies, A. Kairo, and C. L. Bailey.** 1985. Rift Valley fever virus (family Bunyaviridae, genus Phlebovirus). Isolations from Diptera collected during an inter-epizootic period in Kenya. J. Hyg. Cambridge **95:**197–209.
33. **Linthicum, K. J., H. F. Kaburia, F. G. Davies, and K. J. Lindqvist.** 1985. A blood meal analysis of engorged mosquitoes found in Rift Valley fever epizootics area in Kenya. J. Am. Mosquito Control Assoc. **1:**93–95.
34. **Madani, T. A., Y. Y. Al-Mazrou, M. H. Al-Jeffri, A. A. Mishkhas, A. M. Al-Rabeah, A. M. Turkistani, M. O. Al-Sayed, A. A. Abodahish, A. S. Khan, T. G. Ksiazek, and O. Shobokshi.** 2003. Rift Valley fever epidemic in Saudi Arabia: epidemiological, clinical, and laboratory characteristics. Clin. Infect. Dis. **37:**1084–1092.
35. **Mariner, J. C., J. Morrill, and T. G. Ksiazek.** 1995. Antibodies to hemorrhagic fever viruses in domestic livestock in Niger: Rift Valley fever and Crimean-Congo hemorrhagic fever. Am. J. Trop. Med. Hyg. **53:**217–221.
36. **McIntosh, B. M., D. Russell, I. dos Santos, and J. H. Gear.** 1980. Rift Valley fever in humans in South Africa. S. Afr. Med. J. **58**:803–806.
37. **Meegan, J. M., R. H. Watten, and L. W. Laughlin.** 1981. Clinical experience with Rift Valley fever in humans during the 1977 egyptian epizootic. Contrib. Epidemiol. Biostatistics **3:**114–123.
38. **Miller, B. R., M. S. Godsey, M. B. Crabtree, H. M. Savage, Y. Al-Mazrao, M. H. Al-Jeffri, A.-M. M. Abdoon, S. M. Al-Seghayer, A. M. Al-Shahrani, and T. G. Ksiazek.** 2002. Isolation and genetic characterization of Rift Valley fever virus from Aedes vexans arabiensis, Kingdom of Saudi Arabia. Emerg. Infect. Dis. **8:**1492–1494.
39. **Morvan, J., P. E. Rollin, S. Laventure, and J. Roux.** 1992. Duration of immunoglobulin M antibodies against Rift Valley fever virus in cattle after natural infection. Trans. R. Soc. Trop. Med. Hyg. **86:**675.
40. **Nylander, J. A., J. C. Wilgenbusch, D. L. Warren, and D. L. Swofford.** 2008. AWTY (Are We There Yet?): a system for graphical exploration of MCMC convergence in Bayesian phylogenetics. Bioinformatics **24:**581–583.
41. **Posada, D., and K. A. Crandall.** 1998. MODELTEST: testing the model of DNA substitution. Bioinformatics **14:**817–818.
42. **Ramos-Onsins, S. E., and J. Rozas.** 2002. Statistical properties of new neutrality tests against population growth. Mol. Biol. Evol. **19:**2092–2100.
43. **Rogers, A. R., and H. Harpending.** 1992. Population growth makes waves in the distribution of pairwise genetic differences. Mol. Biol. Evol. **9:**552–569.
44. **Ronquist, F., and J. P. Huelsenbeck.** 2003. MrBayes 3: Bayesian phylogenetic inference under mixed models. Bioinformatics **19:**1572–1574.
45. **Sall, A. A., P. M. Zanotto, O. K. Sene, H. G. Zeller, J. P. Digoutte, Y. Thiongane, and M. Bouloy.** 1999. Genetic reassortment of Rift Valley fever virus in nature. J. Virol. **73:**8196–8200.
46. **Sall, A. A., P. M. Zanotto, P. Vialat, O. K. Sene, and M. Bouloy.** 1998. Origin of 1997-98 Rift valley fever outbreak in East Africa. Lancet **352:**1596–1597.
47. **Schmaljohn, C. S., and J. W. Hooper.** 2001. Bunyaviridae: the viruses and their replication, p. 1581–1602. *In* D. M. Knipe, P. M. Howley, D. E. Griffin, R. A. Lamb, M. A. Martin, B. Roizman, and S. E. Straus (ed.), Fields virology, 4th ed. Lippincott Williams & Wilkins, Philadelphia, PA.
48. **Shoemaker, T., C. Boulianne, L. Pezzanite, M. Al-Qahtani, P. E. Rollin, R. Swanepoel, T. G. Ksiazek, and S. T. Nichol.** 2002. Genetic analysis of viruses associated with emergence of Rift Valley fever in Saudi Arabia and Yemen, 2000-01. Emerg. Infect. Dis. **8:**1415–1420.
49. **Suchard, M. A., C. M. Kitchen, J. S. Sinsheimer, and R. E. Weiss.** 2003. Hierarchical phylogenetic models for analyzing multipartite sequence data. Syst. Biol. **52:**649–664.
50. **Suchard, M. A., R. E. Weiss, and J. S. Sinsheimer.** 2001. Bayesian selection of continuous-time Markov chain evolutionary models. Mol. Biol. Evol. **18:**1001–1013.
51. **Suzich, J. A., L. T. Kakach, and M. S. Collett.** 1990. Expression strategy of a Phlebovirus: biogenesis of proteins from the Rift Valley fever virus M segment. J. Virol. **64:**1549–1555.
52. **Swanepoel, R.** 1981. Observations on Rift Valley fever in Zimbabwe. Contrib. Epidemiol. Biostatistics **3:**83–91.
53. **Tajima, F.** 1989. Statistical method for testing the neutral mutation hypothesis by DNA polymorphism. Genetics **123:**585–595.
54. **Towner, J., T. Sealy, T. Ksiazek, and S. Nichol.** 2007. High-throughput molecular detection of hemorrhagic fever virus threats with applications for outbreak settings. J. Infect. Dis. **2007:**S202–S212.
55. **Towner, J. S., M. L. Khristova, T. K. Sealy, M. J. Vincent, B. R. Erickson, D. A. Bawiec, A. L. Hartman, J. A. Comer, S. R. Zaki, U. Stroher, F. Gomes Da Silva, F. del Castillo, P. E. Rollin, T. G. Ksiazek, and S. T. Nichol.** 2006. Marburgvirus genomics and association with a large hemorrhagic fever outbreak in Angola. J. Virol. **80:**6497–6516.
56. **Towner, J. S., P. E. Rollin, D. G. Bausch, A. Sanchez, S. M. Crary, M. Vincent, W. F. Lee, C. F. Spiropoulou, T. G. Ksiazek, M. Lukwiya, F. Kaducu, R. Downing, and S. T. Nichol.** 2004. Rapid diagnosis of Ebola hemorrhagic fever by reverse transcription-PCR in an outbreak setting and assessment of patient viral load as a predictor of outcome. J. Virol. **78:**4330–4341.
57. **Turell, M. J., J. C. Morrill, C. A. Rossi, A. M. Gad, S. E. Cope, T. L. Clements, R. R. Arthur, L. P. Wasieloski, D. J. Dohm, D. Nash, M. M. Hassan, A. N. Hassan, Z. S. Morsy, and S. M. Presley.** 2002. Isolation of West Nile and Sindbis viruses from mosquitoes collected in the Nile Valley of Egypt during an outbreak of Rift Valley fever. J. Med. Entomol. **39:**248–250.
58. **Wilson, A., S. Carpenter, J. Gloster, and P. Mellor.** 2007. Re-emergence of bluetongue in northern Europe in 2007. Vet. Rec. **161:**487–489.
59. **Won, S., T. Ikegami, C. J. Peters, and S. Makino.** 2006. NSm and 78-kilodalton proteins of Rift Valley fever virus are nonessential for viral replication in cell culture. J. Virol. **80:**8274–8278.
60. **Won, S., T. Ikegami, C. J. Peters, and S. Makino.** 2007. NSm protein of Rift Valley fever virus suppresses virus-induced apoptosis. J. Virol. **81:**13335–13345.
61. **Woods, C. W., A. M. Karpati, T. Grein, N. McCarthy, P. Gaturuku, E. Muchiri, L. Dunster, A. Henderson, A. S. Khan, R. Swanepoel, I. Bonmarin, L. Martin, P. Mann, B. L. Smoak, M. Ryan, T. G. Ksiazek, R. R. Arthur, A. Ndikuyeze, N. N. Agata, and C. J. Peters.** 2002. An outbreak of Rift Valley fever in Northeastern Kenya, 1997-98. Emerg. Infect. Dis. **8:**138–144.